



This is a repository copy of *Enhanced tubulation of liposome containing cardiolipin by MamY protein from magnetotactic bacteria.*

White Rose Research Online URL for this paper:
<http://eprints.whiterose.ac.uk/138573/>

Version: Accepted Version

Article:

Tanaka, M., Suwatthanarak, T., Arakaki, A. et al. (5 more authors) (2018) Enhanced tubulation of liposome containing cardiolipin by MamY protein from magnetotactic bacteria. *Biotechnology Journal*. ISSN 1860-6768

<https://doi.org/10.1002/biot.201800087>

This is the peer reviewed version of the following article: Tanaka, M. , Suwatthanarak, T. , Arakaki, A. , Johnson, B. R., Evans, S. D., Okochi, M. , Staniland, S. S. and Matsunaga, T. (2018), Enhanced Tubulation of Liposome Containing Cardiolipin by MamY Protein from Magnetotactic Bacteria. *Biotechnol. J.*, which has been published in final form at <https://doi.org/10.1002/biot.201800087>. This article may be used for non-commercial purposes in accordance with Wiley Terms and Conditions for Self-Archiving.

Reuse

Items deposited in White Rose Research Online are protected by copyright, with all rights reserved unless indicated otherwise. They may be downloaded and/or printed for private study, or other acts as permitted by national copyright laws. The publisher or other rights holders may allow further reproduction and re-use of the full text version. This is indicated by the licence information on the White Rose Research Online record for the item.

Takedown

If you consider content in White Rose Research Online to be in breach of UK law, please notify us by emailing eprints@whiterose.ac.uk including the URL of the record and the reason for the withdrawal request.



eprints@whiterose.ac.uk
<https://eprints.whiterose.ac.uk/>

Research Article

Special issue

AFOB XI: Biomimetic and Bioinspired Biotechnology-Bentley & Gotoh & Martin

Enhanced tubulation of liposome containing cardiolipin by MamY protein from magnetotactic bacteria

Masayoshi Tanaka^{1*}, Thanawat Suwatthanarak¹, Atsushi Arakaki², Benjamin R. G. Johnson³, Stephen D. Evans³, Mina Okochi¹, Sarah Staniland⁴, and Tadashi Matsunaga^{2,5*}

¹Department of Chemical Science and Engineering, Tokyo Institute of Technology, Tokyo, Japan, ²Division of Biotechnology and Life Science, Institute of Engineering, Tokyo University of Agriculture and Technology, Tokyo, Japan, ³School of Physics and Astronomy, University of Leeds, Leeds, UK, ⁴Department of Chemistry, University of Sheffield, Sheffield, UK, ⁵Faculty of Science and Engineering, Waseda University, Tokyo, Japan

Correspondence:

Tadashi Matsunaga, Division of Biotechnology and Life Science, Institute of Engineering, Tokyo university of Agriculture and Technology, 2-24-16 Naka-cho, Koganei, Tokyo 184-8588, Japan. **E-mail:** tmatsuna@cc.tuat.ac.jp

Masayoshi Tanaka, Department of Chemical Science and Engineering, Tokyo Institute of Technology 2-12-1, O-okayama, Meguro-ku, Tokyo 152-8552, Japan. **E-mail:** m_tanaka@chemeng.titech.ac.jp

Keywords: Cardiolipin, Magnetosome, Magnetotactic bacteria, Membrane tubulation, Peptide array

Abbreviations: *M. magneticum* **AMB-1**, *Magnetospirillum magneticum* AMB-1; **BAR**, Bin/amphiphysin/Rvs; **TEM**, Transmission electron microscopy; **CL**, Cardiolipin; **ML**, Liposome made of magnetosome membrane extracted lipids

Abstract

Lipid tubules are of particular interest for many potential applications in nanotechnology. Among various lipid tubule fabrication techniques, the morphological regulation of membrane structure by proteins mimicking biological processes may provide the chances to form lipid tubes with highly-tuned structures. Magnetotactic bacteria synthesize magnetosomes (a unique prokaryotic organelle comprising a magnetite crystal within a lipid envelope). MamY protein has previously been identified as the magnetosome protein responsible for magnetosome vesicle formation and stabilization. Furthermore, MamY has been shown *in vitro* liposome tubulation activity. In this study, the interaction of MamY and phospholipids was investigated by using a lipids-immobilized membrane strip and a peptide array. Here, the binding of MamY to the anionic phospholipid, cardiolipin, was found and enhanced liposome tubulation efficiency. We propose the interaction is responsible for recruiting and locating cardiolipin to elongate liposome *in vitro*. We also suggest a similar mechanism for the invagination site in magnetosomes vesicle formation, where the lipid itself contributes further to increasing the curvature. These findings are highly important to develop an effective biomimetic synthesis technique of lipid tubules and to elucidate the unique prokaryotic organelle formation in magnetotactic bacteria.

1 Introduction

The fabrication of self-assembled lipid nanotubules *in vitro* is an exciting research topic because its applications are diverse. Using unique properties including structural flexibilities (e.g. diameter, length and wall thickness), ease of surface functionalization and biocompatibility, the materials can be used as nanoreactors for functional material synthesis^[1-4], templating the fabrication of biocompatible functional one-dimensional materials^[5-7] and drug carriers^[8-10]. Because of these wide areas of interest, extensive research efforts have been devoted towards finding a means of creating such unique membrane structures *in vitro* and for elucidating the mechanisms of lipid tubule formation.

Various fabrication techniques of lipid tubules have been developed since the first report in 1984^[11] by self-assemble of diacetylene phospholipids. The techniques are generally categorized in two groups: the design of lipid molecules with appropriate structure and compositions for their self-assembling^[12,13], and the morphological regulation by external stimuli such as pulling lipid vesicles with a pipette^[14], electric fields^[15], light irradiation^[16], interaction with cationic particles^[17] and proteins^[18-20]. Among these approaches, the use of proteins mimicking biological systems is potential candidate for a range of lipid tubule formation with both highly-tuned and of more-complicated structures because of the variety of precise protein-regulated membranous structures observed in biology (e.g. endoplasmic reticulum, Golgi network, inner mitochondrial membrane, etc.)^[21-23].

The protein-lipid interaction is an important part of regulating the membranous structure for cellular activity expressions. In eukaryotic cells, the Pleckstrin homology domain in phospholipase C- δ 1 produces a pulling force of membranous structure to form a membrane compartment through the interaction with phosphorylated phosphatidylinositols^[24]. The proteins possessing Bin/amphiphysin/Rvs (BAR) domain

also bound to phosphatidylinositols and the diverse BAR protein family including I-BAR and F-BAR have an important role for membrane invagination processes^[23,25-28]. In prokaryotic cell, while the dynamic organization behaviors of lipid- protein localization for cell division have been investigated^[29-33], research of protein-lipid interaction for prokaryotic organelle formation is lacking thus far.

Magnetotactic bacteria are fascinating to many scientists due to the presence of prokaryotic membranous organelles, called magnetosomes, that comprise a crystalline magnetite core within a lipid envelope, or magnetosome membrane^[34,35]. Previous molecular studies have reported that the complicated biomineralisation process is regulated by a unique set of proteins within the cells^[36-40]. Briefly, magnetosome membranes are formed from cytoplasmic membrane through an invagination process^[36,41] and the vesicles are then aligned along the actin-like filamentous protein^[41-43]. Magnetite crystals are formed within magnetosome vesicles in a highly controlled manner regulated by a suite of magnetosome biomineralisation proteins ^[44-46]. During the organelle formation process, the interaction between specific membrane protein and lipids in the membrane might prove to be pivotal. Our research group has identified a magnetosome membrane protein, MamY, which has been isolated from magnetosome containing small magnetite crystal (presumably in immature stage)^[47]. The *mamY* gene deletion mutant showed the expansion of magnetosome vesicle sizes and the increase of small magnetite crystals, showing MamY's role in the vesicle invagination step. Furthermore, MamY can directly bind to biological membrane vesicles (liposome) and cause the deformation from sphere to tubule *in vitro*^[47]. Therefore, while MamY is hypothesized to be related to the invagination of the magnetosome vesicle, the molecular mechanisms including protein-membrane binding interactions are still unclear.

Here, we investigated the interaction of the MamY protein and a range of lipids by (1) binding assay of MamY protein to various phospholipids, (2) evaluation of liposome

deformation efficiency by MamY protein in the presence of the best binding candidate lipid (cardiolipin (CL)), and (3) binding assay of a series of peptides derived from amino acid sequence of MamY protein to CL. This is the first report showing the direct interaction between a magnetosome membrane protein and specific lipids. The results in this study not only provide the preliminary understanding the presence of a unique protein-lipid interaction is responsible for magnetosome formation in magnetotactic bacteria, but also suggests of how prokaryotic protein could be used to biomimetically synthesize lipid tubule *in vitro*.

2 Materials and methods

2.1 Materials

DOPC (1,2-dioleoyl-sn-glycero-3-phosphocholine, 18:1) and CL (Cardiolipin, 18:1) were purchased from Avanti Polar Lipids, Inc. (Alabaster, AL, USA). Membrane Lipid Strips were obtained from Echelon Bioscience, Inc. (Salt Lake, UT, USA). All other reagents were of the highest commercial grade available. *M. magneticum* AMB-1 (ATCC700264) was cultured anaerobically in magnetic spirillum growth medium (MSGM) in a 8-L fermentor as described previously^[45,48].

2.2 Lipid-strip binding assay

The *mamY* gene was amplified from *M. magneticum* AMB-1 as previously described^[47]. The gene of AmphiphysinBAR protein (human Amphiphysin aa1-239) was cloned into pGEX6p3. Recombinant proteins (MamY and AmphiphysinBAR) were expressed as fusion proteins with glutathione S-transferase (GST) using plasmid vector of pGEX6p-1 and pGEX6p-3, respectively (GE Healthcare Life Sciences, Chicago, Illinois, USA) in *E. coli* BL21. These recombinant proteins were purified with glutathione-sepharose, size-exclusion, and ion-exchange chromatography. Purity (>95%) of these proteins was verified by SDS-PAGE.

For the protein-lipid binding assay, various lipids dotted on strips (Echelon Bioscience Inc., Salt Lake, UT, USA) were blocked with PBS-T buffer (pH 7.4) (137 mM NaCl, 2.7 mM KCl, 4.3 mM Na₂HPO₄, 1.47 mM KH₂PO₄, 0.1% (v/v) Tween-20) supplemented with 3% BSA for 1h with gentle agitation 25°C. After discarding the blocking solution, protein solutions (0.5 µg ml⁻¹ proteins in PBS) were incubated with gentle agitation for 1h at room temperature. The strips were then washed with PBS-T buffer three times with gentle agitation for 5 min each. The washed strips were incubated with mouse anti-GST antibody (GE Healthcare Life Sciences, Chicago, Illinois, USA) for 1 h and washed three times. Anti-mouse IgG-HRP (Horseradish peroxidase) (Thermo Fisher Scientific, Waltham, Massachusetts, USA) was used as a secondary antibody and washed three times. The immunoreactivity was visualized with the ECL detection system (GE Healthcare Life Sciences, Chicago, Illinois, USA).

2.3 Synthesis of peptide arrays

Peptide library of 15-amino-acid peptides was constructed by overlapping 2 amino acids along the sequence of MamY protein and synthesized on cellulose membranes (grade 542; Whatman, Maidstone, UK) activated with β-alanine as N-terminus by peptide auto-spotter (MultiPep Rsi, Intavis AG, Köln, Germany) as shown in previous works [49,50]. It should be noted that the peptide array comprising the 15-mer peptides could reveal the importance of native secondary protein structure^[63]. For the addition of each amino acid, the synthesis cycle began with deprotecting Fmoc-protecting group with 20% piperidine in N,N-dimethylformamide (DMF) before washing the membrane with DMF and ethanol. Prior to amino acid coupling, Fmoc amino acids at 0.5 M were activated by 1.1 M Hydroxybenzotriazole and 1.1 M N,N-diisopropylcarbodiimide. After coupling, the remaining unreacted amino groups were blocked by 4% acetic anhydride in DMF and subsequently washed with DMF and ethanol. The synthesis was conducted according to

manufacturer's instructions with some modifications. After the final cycle, Fmoc and side-chain protecting groups were manually removed with 20% piperidine in DMF and mixture of Milli-Q water, triisopropyl silane and trifluoroacetic acid (2:3:95), respectively. Finally, the membrane was thoroughly washed with dichloromethane, DMF, ethanol and PBS.

2.4 Liposome tubulation assay

Cultured *M. magneticum* AMB-1 cells were resuspended in 10 mM HEPES buffer (pH 7.4) and disrupted twice by French press (2,000 kgf cm⁻³) on ice. After centrifugation, magnetosomes were collected magnetically by a cylindrical Nd-B magnet (15 mm in diameter, 10 mm in height). Total lipids from magnetosome membrane vesicle were extracted according to Bligh and Dyer extraction method^[51]. A liposome tubulation assay was conducted as described previously^[47,52] with minor modifications. Prior to making the liposome solution, glass vials were thoroughly washed with chloroform, methanol, MilliQ and chloroform. After mixing lipid components for liposome formation in chloroform, the solution was dried under argon gas purging and incubated in desiccator for more than 2h. As no tubulation was found for small unilamellar vesicle by MamY protein in our preliminary investigation, giant unilamellar vesicle (GUV) was applied for the tubulation assay. To form GUV, 0.3 M sucrose solution was added in the glass vial containing thoroughly dried lipid cake and were incubated overnight at 37°C. Liposomes (1 mg ml⁻¹ lipid) were then mixed with MamY-GST (final conc.: 30 µM). After incubation for 30 min at 37°C, the samples were spotted onto 150-mesh carbon-coated copper grids (Nisshin EM Co., Tokyo, Japan), stained with 1% (w/v) phosphotungstic acid, and analyzed using JEOL JEM1200EX (JEOL, Tokyo, Japan) operated at an accelerating voltage of 100 kV. To evaluate the tubulation activity of MamY-GST protein in this experimental condition, GST protein was also evaluated as negative control, and no tubulation was found.

2.5 Binding assay between liposome containing CL and peptide array

DOPC, CL and Texas red tagged DHPE (Thermo Fisher Scientific, Waltham, Massachusetts, USA) dissolved in chloroform were mixed with the ratio of 10:1:0.044 for CL-containing DOPC liposome or 10:0:0.04 for DOPC liposome. The mixture was dried under argon gas purging and kept in desiccator for more than 2 h. The obtained lipid cake was hydrated with PBS before 2-min sonication and then 30-s vortex. The lipid solution was extruded through 0.1 μm membrane using an extruder (Avanti Polar Lipids, Inc., Alabama, USA).

The peptide array was blocked with 5% BSA in PBS for 30 min and triplicate washed with 0.05% Tween 20 in PBS for 3 min. The peptide array was soaked into the liposome solution diluted with PBS to 100 $\mu\text{g}/\text{ml}$ for 1 h and triplicate washed with PBS for 3 min. All steps in binding assay were performed at 25°C with gentle agitation. Fluorescence scanning and imaging were performed by biomolecular imager (Typhoon FLA 9500, GE Healthcare, Uppsala, Sweden) using 653 nm excitation wavelength, 669 nm emission light wavelength with LPR filter at 50 mm-pixel size with 500 V. The fluorescence image was quantified by Image Quant software (GE Healthcare, Uppsala, Sweden).

Dissociation constants (K_d) of candidate peptides with CL were determined by binding assay between liposomes and peptide array. The assay was tested at different liposome concentrations ranging from 0 to 150 $\mu\text{g}/\text{ml}$. Fluorescence intensity from binding assay with CL-containing DOPC liposome was subtracted by that with DOPC liposome to specify the binding intensity for CL. Binding curves were drawn between blank-subtracted intensity and CL concentration for K_d determination. Langmuirian binding isotherm equation $\{Y = B_{\text{max}} \times X / (K_d + X)\}$ was used, where Y was blank-subtracted intensity, X was concentration of CL, and B_{max} was the intensity at saturation. All K_d values were calculated from SigmaPlot 11.0 software (Systat Software Inc., California, USA).

To confirm the binding between candidate peptide and CL, binding assay by surface plasmon resonance (SPR) system (Biacore X100 Plus Package, GE Healthcare, Uppsala, Sweden) was conducted. AAFGKLNSASRAALI or AAAA peptide dissolved in acetate pH 5.5 to 0.5 mg/ml was immobilized on CM5 sensor chip surface using amine coupling kit at 5 μ l/min for 18 min. The immobilized response was around 300 and 200 RU for AAFGKLNSASRAALI and AAAA peptide, respectively. For binding analysis, the analyte, 10% CL-containing DOPC liposomes or DOPC liposomes diluted with HBS-EP buffer to 1 mg/ml, was applied at a flow rate of 10 μ l/min for 180 s followed by 600 s of dissociation time. After each binding analysis, the surface was regenerated by 10 mM glycine-HCl pH 2.0 at a flow rate of 10 μ l/min for 1 min.

3 Results

3.1 Binding assay between MamY protein and various phospholipids using membrane lipid array

To test whether MamY can bind to specific phospholipids, MamY-GST and a series of phospholipids were used to conduct a protein-lipid overlay binding assay. As shown in Fig. 1, unexpectedly, the unique binding properties of MamY protein to CL and 3-sulfogalactosylceramide (sulfatide) were clearly observed by chemiluminescence detection (Fig. 1a), while no binding to other phospholipids including the major lipid components (PE; phosphatidylethanolamine, PS; phosphatidylserine, and PC; phosphatidylcholin) in the magnetosome membrane of *M. magneticum* AMB-1^[36] were found. On the other hand, BAR domain of human Amphiphysin (AmphiphysinBAR, control) bound to phosphatidylinositols [PtdIns(4)P, PtdIns(4,5)P₂, and PtdIns(3,4,5)P₃], sulfatide, phosphatidic acid, phosphatidylserine (PS), phosphatidylethanolamine (PE), phosphatidylglycerol (PG) and CL (Fig. 1b), while the negative control (GST) showed no binding ability to any lipids on the lipid array as also reported previously^[53] (Fig. 1c).

Among a range of negatively charged lipids in the strip, only two negatively charged lipids (CL and sulfatide) showed binding to MamY protein. The observation suggested that although a negative charge is essential, the interaction is not derived simple from electrostatic interaction. The unique feature of protein binding specifically to CL and Sulfatide has previously been reported for α -helices regions in some proteins^[54,55]. While the binding mechanism is still unclear in these proteins, similar interaction may contribute to the binding here because the MamY protein is also predicted to be dominant by α -helices regions^[47]. Sulfatide is the major acidic glycosphingolipid in central and peripheral nerve myelin in mammals^[56]. As the lipid group of glycosphingolipids including Sulfatide is generally synthesized only in eukaryotic cell with a few exceptions^[57,58], we focused on the interaction between MamY and CL in the following experiments.

3.2 Tubulation assay of liposome containing CL by MamY protein

MamY has been previously shown to have deformation function of liposomes from spherical to tubulated morphology^[47]. As the interaction between MamY and CL was confirmed in this study, as the next step, it was investigated whether the interaction enhances the liposome tubulation *in vitro*. In the presence of MamY-GST protein, liposome tubulation was clearly observed, while liposomes were spherical morphologies in the absence of MamY (Fig. 2). In addition, as found in Table 1, the tubulation efficiency was increased according to the increase of CL concentration. When the liposome was made of pure magnetosome membrane lipids (ML), the tubulation efficiency was 3.3%. It notes that the GST fusion to MamY protein seems to little effect on the liposome tubulation activity because the tubulation activity of MamY-GST (3.3%) was similar level with MamY without GST tag (approximately 4%)^[47]. GST protein also showed no liposome tubulation activity. At 5%, 10% and 20% of CL, a tubulation efficiency of approximately 20% was reached. This result demonstrated that MamY interacts with CL, and the interaction is

associated with liposome tubulation. The tubulation efficiency of liposome comprising magnetosome lipids supplemented with CL seems to be maximum at approximately 20%, and all MamY molecule seems to be used for the tubulation of liposome containing more than 5% of CL.

3.3 Binding assay between MamY derived peptides and CL containing liposome using peptide array

To begin to understand the location of the CL binding region and mechanism of how MamY binds to CL, a 15-mer peptide library (188 peptides) constructed by overlapping 2 amino acids along the sequence of MamY protein (389 amino acids) was synthesized (Fig. 3a). A binding assay of this array to CL-containing DOPC liposome and DOPC liposome (control) was performed (Fig. 3). Some peptide spots showed higher intensity with CL-containing DOPC liposome than DOPC liposome (Fig. 3b). In addition, previously reported CL binding peptide^[59](shown as “C” peptide in Fig. 3b), KNKEKK, shows binding only for CL-containing DOPC liposome. In order to quantitatively evaluate the binding to CL, the fluorescence intensity profile of DOPC liposome was subtracted from CL containing DOPC liposome (Fig. 3c). Herein, 8 peptides having greater intensity than average (+ 2SD value were selected as CL binding peptides (Table 2)) and the intensity was remarkably higher than the control peptide. SPR experiment using a screened CL binding candidate peptide (AAFGKLN SASRAALI) and tetra-alanine peptide (negative control) was applied to confirm the results from binding assay. In this assay, each peptide was immobilized on a sensor chip surface, and subsequently the solution containing liposome was flowed to observe the bound mass proportion on the surface along time. From blank-subtracted SPR sensor-gram, the bound mass or response on AAFGKLN SASRAALI peptide-immobilized surface was larger when CL-containing DOPC liposome was flowed (Supplementary figure 1-a). From this data, strong binding activity of

screened peptide to CL was clearly confirmed by comparison with only DOPC liposomes. In contrast, AAAA peptide-immobilized surface display insignificant difference with the both types of liposome (Supplementary figure 1-b). In addition, a protein region from aa280 to aa339 seems to be important for CL binding because 4 peptides were collectively found. As the peptides had a wide range of isoelectric point (pI) from 4.53 to 11.54 and of the GRAVY (grand average of hydropathy) value from -1.91 to 0.67, various types of interaction to CL in each peptide may occur.

The dissociation constant (K_d) of 8 candidate peptides (named p1-p8) to CL along with control peptide were determined by binding assay with CL-containing DOPC liposome and DOPC liposome using peptide array. By using the Langmuirian binding isotherm equation (see materials and methods), each K_d value of candidate peptides to CL was calculated (Table 2) (Supplementary figure 2). All candidate peptides except p2 have stronger affinity to CL than control peptide (KNKEKK, $K_d=9.49 \mu\text{M}$) in this experimental condition. Among these peptides, p6 (RKFISTLTTAYFAGD) showed the strongest affinity to CL ($K_d=0.65 \mu\text{M}$). The pI (8.59), GRAVY (0.07) and net charge (+1) were relatively neutral in this CL binding peptide candidates.

4 Discussion

In this study, the interaction between a prokaryotic membrane deformation protein, MamY, and CL was found. From the binding assay between CL and peptide library derived from MamY amino acid sequence, some peptides were suggested to play an important role for the interaction. This is the first report showing the direct interaction between magnetosome membrane protein and specific lipid. Furthermore, by the supplementation of CL to liposome, the effective liposome tubulation condition was developed.

Binding of MamY protein to negatively charged CL was disclosed in this study. In this experimental condition (pH=7.4), the protein (pI=5.38) seems to be a generally negatively charged molecule. This is interesting because the result suggests that the interaction is not simply derived from electrostatic interaction as a whole protein molecule. By evaluation of binding between peptide sequences derived from MamY and CL, as all 8 peptides included positively charged amino acids (R or K) and hydrophobic amino acids (e.g., V, I, L)(Table 2), both of the electrostatic and hydrophobic interaction seem to be contributed for the binding to CL. A lipid 4 is a dynamic environment with varying properties ranging from nonpolar within the hydrocarbon chain to polar at the headgroup-solution interface. Therefore, by the interactions between various amino acids within the screened peptides and the counterpart within CL molecule, the selective binding might reveal. In addition, it is reported that some α -helix repeat structure within the protein relate to the stable binding to other biological membranes and its deformation^[60,61], the structural feature of MamY protein comprising of repeat of α -helix may also contribute to the stable binding to CL. In fact, all 8 candidate peptides were found in α -helix regions of MamY protein predicted by PSIPRED(<http://bioinf.cs.ucl.ac.uk/psipred/>)^[62](Supplementary figure 2). On the other hand, since there is no report about 3D structure of MamY protein thus far, it is still unclear whether these peptides interact at plural sites or at nearby sites in the protein structure. Further study including protein structural analysis should be addressed to fully understand the molecular mechanism of magnetosome vesicle regulation by MamY protein.

The supplementation of CL in liposome enhanced the tubulation efficiency by MamY protein, but the mechanism of liposome tubulation is still unclear. CL is an anionic tetraacylphospholipid which is almost exclusively confined to the innermitochondrial membrane in eukaryotic cells, whereas in prokaryotes, it has been identified in the

cytoplasmic membrane. For example, CL-enriched membrane domains were reported in bacterial cells, *E. coli*^[29,30], *Bacillus subtilis*^[64] and *Pseudomonas putida*^[65]. As a result of its conical shape, CL employs lateral pressure on a membrane containing other phospholipids, and results in membrane curvature formation. In fact, in *E. coli* cells, CL is localized at the cell poles due to the membrane curvature^[29,30]. As the size of magnetosome vesicle is approximately 100 nm, the membrane seems to be one of the most highly-curved membrane structure in magnetotactic bacteria. Therefore, MamY may play important role for the recruitment of CL to magnetosomes in order to induce the formation of highly-curved vesicle formation and/or stabilization of the structure. The hypothesis is also supported by the bioinformatics analysis. Based on the protein domain analysis of MamY by Pfam^[47], p4 and p7 are expected to have a similarity with caspase recruitment domain^[66], involving in apoptotic signaling and requiring CL as a binding platform to recruit apoptotic factors^[67]. In addition, based on the proteomic and genomic studies in magnetotactic bacteria, dozens of proteins including filamentous MamK protein and functionally unclear proteins have been suggested to play important roles for magnetosome formation^[36,39,40,68,69]. In eukaryotic cells, as BAR protein regulates the intracellular vesicle formation cooperated with filamentous actin protein and with various proteins^[70], MamY protein may also work for magnetosome vesicle formation cooperated with other magnetosome proteins. By the utilization of these proteins with MamY, liposome tubulation efficiency may improve. As reported in the literatures about liposome tubulation protein analyses^[28,52,71-73], further investigations of MamY function in both *in vivo* and *in vitro* studies including the dynamics analysis of each lipid and protein molecules by real time monitoring during liposome tubulation, protein structural analysis and detail TEM image analysis of tubulated liposome will clarify the importance of this interaction in liposome tubulation and in magnetosome formation of magnetotactic bacteria.

In summary, the interaction of MamY protein and the partial amino acid sequences of MamY with CL was demonstrated in this study. In addition, the supplementation of CL into liposome revealed the enhancement of lipid tubulation efficiency by MamY protein. The results in this manuscript not only give us the hint to effectively synthesize lipid tubule by prokaryotic protein but also might suggest the presence of unique protein-lipid interaction for magnetosome formation in magnetotactic bacteria. The liposome tubulation event, investigated in this study, was induced by the external stimuli of protein addition. This technique could be useful tool for elucidation of biological reactions onto/within membrane structures with different curvature. In addition, although the synthesis efficiency of lipid tubule is still low (approximately 20%), the synthesized materials with unique characteristics, such as biocompatibility, high dispersibility, and the potential of diameter tuning with a further molecular engineering technique, could be useful for various applications in nanobiotechnology.

Acknowledgement

This work was supported by JSPS KAKENHI (Grant Numbers: 16K14488, 16H02421 and 15H04192). M.T. thanks for funds from Foundation for Promotion of Material Science and Technology (MST) of Japan and the Royal Society UK under the Newton International Fellowships follow on funding scheme. And this work was supported in part by the international collaboration research projects sponsored by the JSPS and the Royal Society. We thank Prof. Naoki Mochizuki and Dr. Michitaka Masuda for kindly providing plasmid pGEX6p3-AmphiphysinBAR (aa1-239). This paper is dedicated to Prof. Stephen Baldwin who contributed greatly to the conceptualization and initial experiments of this study. He is greatly missed.

Conflict of interest

The authors declare no financial or commercial conflict of interest.

5 References

- [1] B. Yang, S. Kamiya, K. Yoshida, T. Shimizu, *Chem. Commun. (Camb)*. **2004**, 500–501.
- [2] Y. Zhou, M. Kogiso, C. He, Y. Shimizu, N. Koshizoki, T. Shimizu, *Adv. Mater.* **2007**, *19*, 1054–1058.
- [3] I. Kim, Y. H. Park, D. A. Rey, C. A. Batt, *J. Drug Target.* **2008**, *16*, 716–722.
- [4] S. Baral, P. Schoen, *Chem. Mater.* **1993**, *5*, 145–147.
- [5] M. Tanaka, K. Critchley, T. Matsunaga, S. D. Evans, S. S. Staniland, *Small* **2012**, *8*, 1590–1595.
- [6] A. J. Patil, E. Muthusamy, A. M. Seddon, S. Mann, *Adv. Mater.* **2003**, *15*, 1816–1819.
- [7] T. Shimizu, in *J. Polym. Sci. Part A Polym. Chem.*, **2006**, pp. 5137–5152.
- [8] Y. Zhou, *Crit. Rev. Solid State Mater. Sci.* **2008**, *33*, 183–196.
- [9] N. Kameta, H. Minamikawa, M. Masuda, G. Mizuno, T. Shimizu, *Soft Matter* **2008**, *4*, 1681.
- [10] J. M. Schnur, R. Price, A. S. Rudolph, *J. Control. Release* **1994**, *28*, 3–13.
- [11] P. Yager, P. E. Schoen, *Mol. Cryst. Liq. Cryst.* **1984**, *106*, 371–381.
- [12] J. P. Douliez, C. Gaillard, L. Navailles, F. Nallet, *Langmuir* **2006**, *22*, 2942–2945.
- [13] S. Kamiya, H. Minamikawa, J. H. Jung, B. Yang, M. Masuda, T. Shimizu, *Langmuir* **2005**, *21*, 743–750.
- [14] M. Heinrich, A. Tian, C. Esposito, T. Baumgart, *Proc. Natl. Acad. Sci.* **2010**, *107*, 7208–7213.
- [15] H. Bi, D. Fu, L. Wang, X. Han, *ACS Nano* **2014**, *8*, 3961–3969.
- [16] C. Pernpeintner, J. A. Frank, P. Urban, C. R. Roeske, S. D. Pitzl, D. Trauner, T. Lohmüller, *Langmuir* **2017**, *33*, 4083–4089.
- [17] Y. Yu, S. Granick, *J. Am. Chem. Soc.* **2009**, *131*, 14158–14159.

- [18] M. Masuda, S. Takeda, M. Sone, T. Ohki, H. Mori, Y. Kamioka, N. Mochizuki, *EMBO J.* **2006**, *25*, 2889–2897.
- [19] J. C. Stachowiak, C. C. Hayden, D. Y. Sasaki, *Proc. Natl. Acad. Sci.* **2010**, *107*, 7781–7786.
- [20] N. Gopaldass, B. Fauvet, H. Lashuel, A. Roux, A. Mayer, *EMBO J.* **2017**, e201796859.
- [21] B. Tandler, C. L. Hoppel, J. A. Mears, *Antioxidants* **2018**, *7*, 30.
- [22] W. J. Nicolas, M. S. Grison, E. M. Bayer, *J. Exp. Bot.* **2018**, *69*, 91–103.
- [23] M. M. Kozlov, F. Campelo, N. Liska, L. V. Chernomordik, S. J. Marrink, H. T. McMahon, *Curr. Opin. Cell Biol.* **2014**, *29*, 53–60.
- [24] M. J. Scholze, K. S. Barbieux, A. De Simone, *bioRxiv* **2017**, 215079.
- [25] W. Zhao, L. Hanson, H. Y. Lou, M. Akamatsu, P. D. Chowdary, F. Santoro, J. R. Marks, A. Grassart, D. G. Drubin, Y. Cui, et al., *Nat. Nanotechnol.* **2017**, *12*, 750–756.
- [26] T. Hirama, S. M. Lu, J. G. Kay, M. Maekawa, M. M. Kozlov, S. Grinstein, G. D. Fairn, *Nat. Commun.* **2017**, *8*, 1393.
- [27] Y. F. Barooji, A. Rørvig-Lund, S. Semsey, S. N. S. Reihani, P. M. Bendix, *Sci. Rep.* **2016**, *6*, 30054.
- [28] Y. Tanaka-Takiguchi, T. Itoh, K. Tsujita, S. Yamada, M. Yanagisawa, K. Fujiwara, A. Yamamoto, M. Ichikawa, K. Takiguchi, *Langmuir* **2013**, *29*, 328–336.
- [29] G. Carranza, F. Angius, O. Illoaia, A. Solgadi, B. Miroux, I. Arechaga, *Biochim. Biophys. Acta - Biomembr.* **2017**, *1859*, 1124–1132.
- [30] T. Romantsov, K. Gonzalez, N. Sahtout, D. E. Culham, C. Coumoundouros, J. Garner, C. H. Kerr, L. Chang, R. J. Turner, J. M. Wood, *Mol. Microbiol.* **2018**, *107*, 623–638.
- [31] P. C. Hsu, F. Samsudin, J. Shearer, S. Khalid, *J. Phys. Chem. Lett.* **2017**, *8*, 5513–5518.
- [32] L. D. Renner, D. B. Weibel, *J. Biol. Chem.* **2012**, *287*, 38835–38844.
- [33] L. D. Renner, D. B. Weibel, *Proc. Natl. Acad. Sci.* **2011**, *108*, 6264–6269.
- [34] Y. A. Gorby, T. J. Beveridge, R. P. Blakemore, *J. Bacteriol.* **1988**, *170*, 834–841.

- [35] R. Blakemore, *Science* **1975**, *190*, 377–9.
- [36] M. Tanaka, Y. Okamura, A. Arakaki, T. Tanaka, H. Takeyama, T. Matsunaga, *Proteomics* **2006**, *6*, 5234–5247.
- [37] T. Matsunaga, M. Nemoto, A. Arakaki, M. Tanaka, *Proteomics* **2009**, *9*, 3341–3352.
- [38] K. Grünberg, E. Müller, A. Otto, R. Reszka, D. Linder, M. Kube, R. Reinhardt, Schüler D., *Appl. Environ. Microbiol.* **2004**, *70*, 1040–1050.
- [39] D. Murat, A. Quinlan, H. Vali, A. Komeili, *Proc. Natl. Acad. Sci. U. S. A.* **2010**, *107*, 5593–5598.
- [40] A. Lohße, S. Borg, O. Raschdorf, I. Kolinko, E. Tompa, M. Pósfai, D. Faivre, J. Baumgartner, D. Schüler, *J. Bacteriol.* **2014**, *196*, 2658–2669.
- [41] A. Komeili, Z. Li, D. K. Newman, G. J. Jensen, *Science* **2006**, *311*, 242–245.
- [42] A. Scheffel, D. Schüler, *J. Bacteriol.* **2007**, *189*, 6437–6446.
- [43] O. Draper, M. E. Byrne, Z. Li, S. Keyhani, J. C. Barrozo, G. Jensen, A. Komeili, *Mol. Microbiol.* **2011**, *82*, 342–354.
- [44] A. Arakaki, J. Webb, T. Matsunaga, *J. Biol. Chem.* **2003**, *278*, 8745–8750.
- [45] A. Yamagishi, M. Tanaka, J. J. M. Lenders, J. Thiesbrummel, N. A. J. M. Sommerdijk, T. Matsunaga, A. Arakaki, *Sci. Rep.* **2016**, *6*, 29785.
- [46] A. Arakaki, A. Yamagishi, A. Fukuyo, M. Tanaka, T. Matsunaga, *Mol. Microbiol.* **2014**, *93*, 554–567.
- [47] M. Tanaka, A. Arakaki, T. Matsunaga, *Mol. Microbiol.* **2010**, *76*, 480–488.
- [48] M. Tanaka, Y. Nakata, T. Mori, Y. Okamura, H. Miyasaka, H. Takeyama, T. Matsunaga, *Appl. Environ. Microbiol.* **2008**, *74*, 3342–3348.
- [49] M. Tanaka, S. Hikiba, K. Yamashita, M. Muto, M. Okochi, *Acta Biomater.* **2017**, *1*, 13–26.
- [50] M. Okochi, M. Muto, K. Yanai, M. Tanaka, T. Onodera, J. Wang, H. Ueda, K. Toko, *ACS Comb. Sci.* **2017**, *19*, 625–632.

- [51] E. G. Bligh, W. J. Dyer, *Can. J. Biochem. Physiol.* **1959**, *37*, 911–917.
- [52] K. Takei, V. I. Slepnev, V. Haucke, P. De Camilli, *Nat. Cell Biol.* **1999**, *1*, 33–39.
- [53] L. A. Gish, J. M. Gagne, L. Han, B. J. DeYoung, S. E. Clark, *PLoS One* **2013**, *8*, DOI 10.1371/journal.pone.0066345.
- [54] N. B. Ray, L. Durairaj, B. B. Chen, B. J. McVerry, A. J. Ryan, M. Donahoe, A. K. Waltenbaugh, C. P. O'Donnell, F. C. Henderson, C. A. Etscheidt, et al., *Nat. Med.* **2010**, *16*, 1120–1127.
- [55] M. Desmurs, M. Foti, E. Raemy, F. M. Vaz, J.-C. Martinou, A. Bairoch, L. Lane, *Mol. Cell. Biol.* **2015**, *35*, 1139–1156.
- [56] K.-A. Nave, H. B. Werner, *Annu. Rev. Cell Dev. Biol.* **2014**, *30*, 503–533.
- [57] Y. Kinjo, D. Wu, G. Kim, G. W. Xing, M. A. Poles, D. D. Ho, M. Tsuji, K. Kawahara, C. H. Wong, M. Kronenberg, *Nature* **2005**, *434*, 520–525.
- [58] D. Balkwill, J. K. Fredrickson, M. F. Romine, *Prokaryotes SE - 23* **2006**, 605–629.
- [59] Y. Sheng, A. Sali, H. Herzog, J. Lahnstein, S. A. Krilis, *J Immunol* **1996**, *157*, 3744–3751.
- [60] A. Shimada, H. Niwa, K. Tsujita, S. Suetsugu, K. Nitta, K. Hanawa-Suetsugu, R. Akasaka, Y. Nishino, M. Toyama, L. Chen, et al., *Cell* **2007**, *129*, 761–772.
- [61] C. M. Khursigara, X. Wu, P. Zhang, J. Lefman, S. Subramaniam, *Proc. Natl. Acad. Sci. U. S. A.* **2008**, *105*, 16555–16560.
- [62] D. T. Jones, *J. Mol. Biol.* **1999**, *292*, 195–202.
- [63] C. Katz, L. Levy-Beladev, S. Rotem-Bamberger, T. Rito, S. G. D. Rüdiger, A. Friedler, *Chem. Soc. Rev.* **2011**, *40*, 2131–2145.
- [64] T. Doan, J. Coleman, K. A. Marquis, A. J. Meeske, B. M. Burton, E. Karatekin, D. Z. Rudner, *Genes Dev.* **2013**, *27*, 322–334.
- [65] P. Bernal, J. Muñoz-Rojas, A. Hurtado, J. L. Ramos, A. Segura, *Environ. Microbiol.* **2007**, *9*, 1135–1145.

- [66] R. D. Finn, P. Coggill, R. Y. Eberhardt, S. R. Eddy, J. Mistry, A. L. Mitchell, S. C. Potter, M. Punta, M. Qureshi, A. Sangrador-Vegas, et al., *Nucleic Acids Res.* **2016**, *44*, D279–D285.
- [67] J. Dudek, *Front. Cell Dev. Biol.* **2017**, *5*, 90.
- [68] A. Arakaki, D. Kikuchi, M. Tanaka, A. Yamagishi, T. Yoda, T. Matsunaga, *J. Bacteriol.* **2016**, JB.00280-16.
- [69] T. Matsunaga, Y. Okamura, Y. Fukuda, A. T. Wahyudi, Y. Murase, H. Takeyama, *DNA Res.* **2005**, *12*, 157–166.
- [70] T. Nishimura, N. Morone, S. Suetsugu, *Biochem. Soc. Trans.* **2018**, *46*, 379–389.
- [71] M. Moniruzzaman, M. Z. Islam, S. Sharmin, H. Dohra, M. Yamazaki, *Biochemistry* **2017**, *56*, 4419–4431.
- [72] Y. Yamashita, S. M. Masum, T. Tanaka, M. Yamazaki, *Langmuir* **2002**, *18*, 9638–9641.
- [73] T. Wollert, C. Wunder, J. Lippincott-Schwartz, J. H. Hurley, *Nature* **2009**, *458*, 172–177.

Table 1. Evaluation of liposome tubulation activity in the presence of CL.

Magnetosome lipid : Cardiolipin	Tubulated/Observed	Efficiency (%)
100 : 0	6/183	3.3
97.5 : 2.5	13/175	7.4
95 : 5	41/203	20.2
90 : 10	38/224	17.0
80 : 20	33/179	18.4
100 : 0 (no protein)	0/168	0.0
90 : 10 (no protein)	0/170	0.0

Table 2. Characteristics of CL binding peptides obtained from MamY amino acid sequence.

Name	Peptide number	Sequence	Subtracted intensity ^{a)} (a.u. $\times 10^5$)	pI ^{b)}	GRAVY ^{c)}	Charge ^{d)}	K _d (μ M)
p1	10	AAFGKLNLSASRAALI	2.71 \pm 0.18	11.00	0.67	+2	4.75 \pm 0.78
p2	142	FISTLTTAYFAGDKN	2.34 \pm 0.42	5.83	0.13	0	11.97 \pm 5.22
p3	155	NRSEQLRRCAEDTES	2.08 \pm 0.26	4.87	-1.91	-1.1	1.62 \pm 0.61
p4	105	RVLSQEITQELSQIT	2.04 \pm 0.45	4.53	-0.28	-1	2.02 \pm 0.47
p5	163	RQQISKILREAREIR	1.94 \pm 0.27	11.54	-1.17	+3	1.19 \pm 0.19
p6	141	RKFISTLTTAYFAGD	1.92 \pm 0.22	8.59	0.07	+1	0.65 \pm 0.31
p7	104	SQRVLSQEITQELSQ	1.56 \pm 0.17	4.53	-0.82	-1	1.36 \pm 0.33
p8	26	GWKNLFTMLPHEFFI	1.55 \pm 0.14	6.75	0.31	+0.1	2.31 \pm 0.37
C	C	KNKEKK	0.45 \pm 0.11	10.0	-3.77	+3	9.49 \pm 3.58

a) The fluorescence intensity was shown from the intensity of CL containing DOPC liposome subtracted with DOPC liposome. b), c) and d) were analyzed using the ProtParam tool in ExpASY (<http://web.expasy.org/protparam/>).

Figure legends

Figure 1. Dot-blot assay of MamY protein for the interactions with phospholipids.

Nitrocellulose-immobilized phospholipids at 100 pmol per spot were incubated with 0.5 $\mu\text{g ml}^{-1}$ of proteins (a; MamY-GST, b; AmphiphysinBAR-GST, and c; GST). Top image shows the lipid profiles in array. Binding of proteins was detected by anti-GST HRP conjugated antibody with chemiluminescent substrate.

Figure 2. Liposome tubulation assay with MamY protein. Representative electron micrographs of the magnetosome membrane extracted lipid liposome (ML) with CL supplementation (5%) (right) and without the supplementation (left) before (top) and after (middle) the MamY protein addition at 30 μM . The bottom images were enlarged from the square region in middle images to show the lipid tubule structure.

Figure 3. Evaluation of CL binding property in peptide library comprising partial sequences in amino acid sequence of MamY protein by using the peptide array.

Designed peptide array a) and the fluorescent images of peptide arrays after binding with b-1) CL containing DOPC liposome and b-2) only DOPC liposome. c) Fluorescent intensity profile of each peptide spot; the intensity from CL containing DOPC liposome was subtracted from the intensity of only DOPC liposome. Error bar indicates SD derived from triple results.

Supplementary figure 1. Blank-subtracted SPR sensorgrams of binding analysis from a) AAFGKLNSASRAALI peptide-immobilized chip and b) AAAA peptide-immobilized chip in case of flowing 10% CL-containing DOPC liposome and DOPC liposome. The contact time is 180 s. The higher response could be seen when CL-containing liposome was flowed over AAFGKLNSASRAALI peptide-immobilized chip.

Supplementary figure 2. Evaluation of dissociation constant (K_d) of 8 CL binding peptide candidates using peptide array. Synthesized peptide arrays were incubated in the solution containing DOPC with CL and without CL. a) The top images show the peptide array after binding assay with different concentration of liposome. b) In order to obtain the K_d value of candidate peptides to CL, subtracted fluorescence intensities were plotted from the different intensities between binding assays with CL-containing DOPC liposome and DOPC liposome. Error bar indicates standard deviation (SD) derived from triple results.

Supplementary figure 3. Predicted secondary structure of MamY protein by PSIPRED with identified CL binding peptide regions. Screened peptides as CL binder were underlined.

Triglyceride	○	○	PtdIns
Diacylglycerol (DAG)	○	○	PtdIns(4)P
Phosphatidic Acid (PA)	○	○	PtdIns(4,5)P ₂
Phosphatidylserine (PS)	○	○	PtdIns(3,4,5)P ₃
Phosphatidylethanolamine (PE)	○	○	Cholesterol
Phosphatidylcholine (PC)	○	○	Sphingomyelin
Phosphatidylglycerol (PG)	○	○	Sulfatide
Cardiolipin (CL)	○	○	Solvent Blank

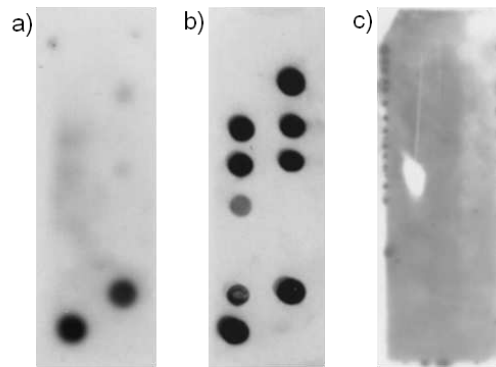


Fig. 1 Tanaka et al.

Figure 1. Dot-blot assay of MamY protein for the interactions with phospholipids.

Nitrocellulose-immobilized phospholipids at 100 pmol per spot were incubated with 0.5 $\mu\text{g ml}^{-1}$ of proteins (a; MamY-GST, b; AmphiphysinBAR-GST, and c; GST). Top image shows the lipid profiles in array. Binding of proteins was detected by anti-GST HRP conjugated antibody with chemiluminescent substrate.

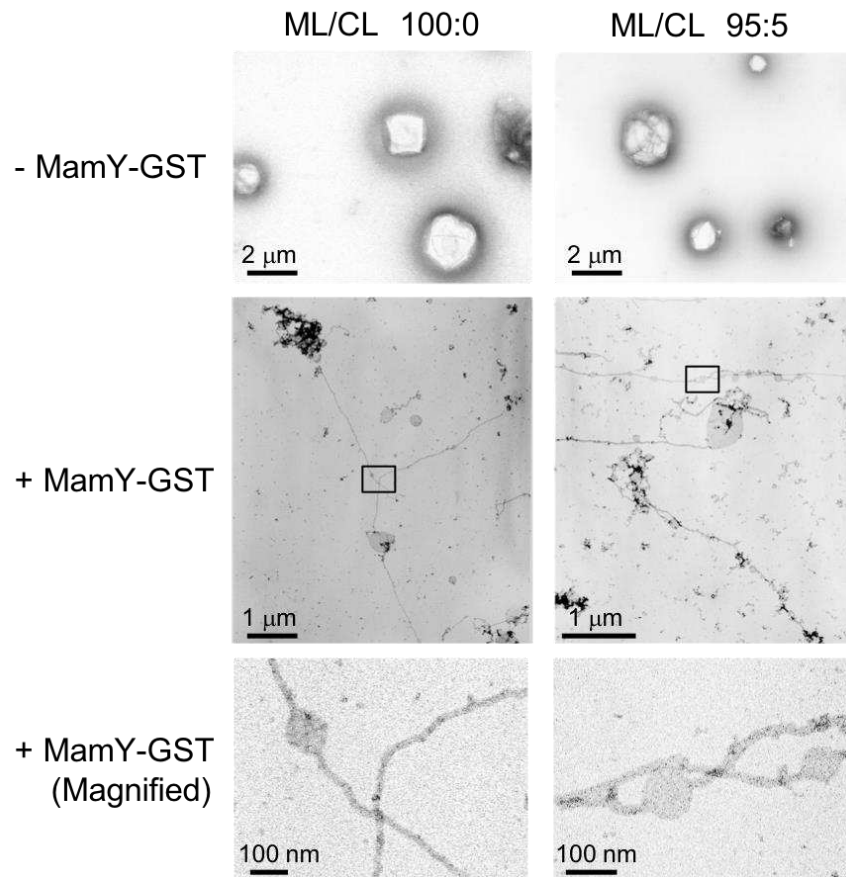
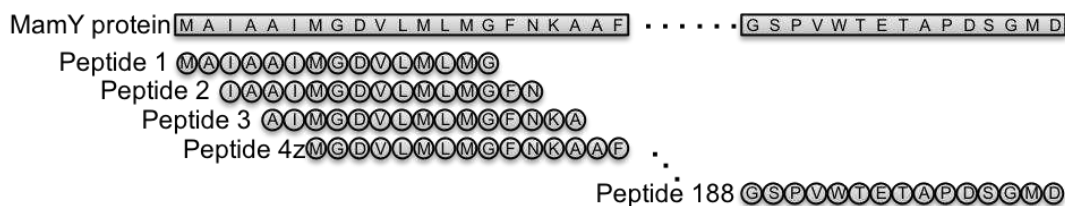


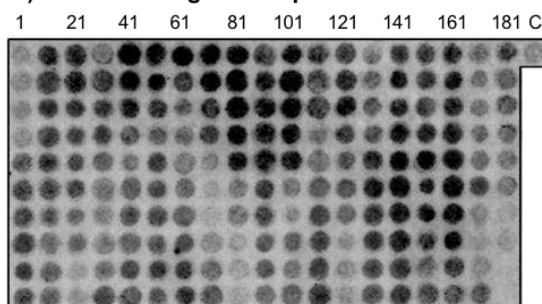
Fig. 2 Tanaka et al.

Figure 2. Liposome tubulation assay with MamY protein. Representative electron micrographs of the magnetosome membrane extracted lipid liposome (ML) with CL supplementation (5%) (right) and without the supplementation (left) before (top) and after (middle) the MamY protein addition at 30 μ M. The bottom images were enlarged from the square region in middle images to show the lipid tubule structure.

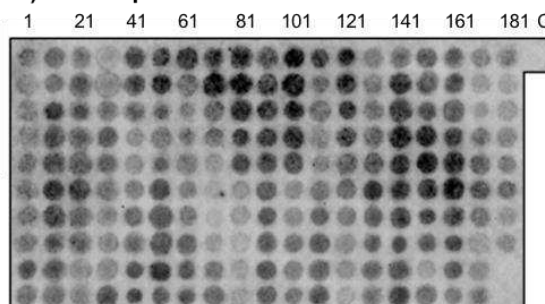
a) Schematic illustration of peptide array design from MamY protein amino acid sequence



b-1) CL containing DOPC liposome



b-2) DOPC liposome



c) Quantitative evaluation of CL binding peptide using peptide array

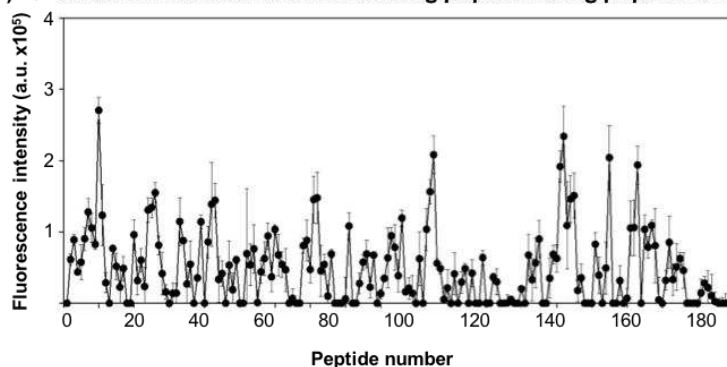


Fig. 3 Tanaka et al.

Figure 3. Evaluation of CL binding property in peptide library comprising partial

sequences in amino acid sequence of MamY protein by using the peptide array.

Designed peptide array a) and the fluorescent images of peptide arrays after binding with

b-1) CL containing DOPC liposome and b-2) only DOPC liposome. c) Fluorescent intensity

profile of each peptide spot; the intensity from CL containing DOPC liposome was

subtracted from the intensity of only DOPC liposome. Error bar indicates SD derived from

triple results.